ACS OMEGA

ACS AUTHORCHOICE

http://pubs.acs.org/journal/acsodf

Article

Liposomal Dendritic Cell Vaccine in Breast Cancer Immunotherapy

Hong Pan,[‡] Hongyan Shi,[‡] Peng Fu, Pengfei Shi, and Jianyuan Yang*

Cite This: *ACS Omega* 2021, 6, 3991−3998

Read Online

ACCESS | Metrics & More | Article Recommendations

ABSTRACT: Cancer vaccine is well recognized as a promising approach for immunotherapy of cancers. Since dendritic cells (DCs) are capable of processing and presenting antigens to initiate the immune response cascade, the development of DC vaccines is considered as a good choice for the treatment of cancer. Herein, a folic acid (FA)-modified liposome was constructed and loaded with chlorin e6 (Ce6) as a DC vaccine (FA-Lipo-Ce6). It was suggested that the loaded Ce6 within FA-Lipo-Ce6 can be activated under laser irradiation. The photodynamic therapy (PDT) of Ce6 was expected to create on-demand reactive oxygen species (ROS) in situ, which causes cell death and trigger the exposure of tumor-associated antigen (TAA). In addition, the produced ROS can mimic the inflammatory responses for the employment of DC for better antigen presentation and immune response. Most importantly, the employment of DC can recognize the exposed TAA to stimulate DC for effective vaccination in situ. Our results demonstrated the powerful capacity of FA-Lipo-Ce6 to induce DC activation, leading to effective suppression of the growth of breast cancers.

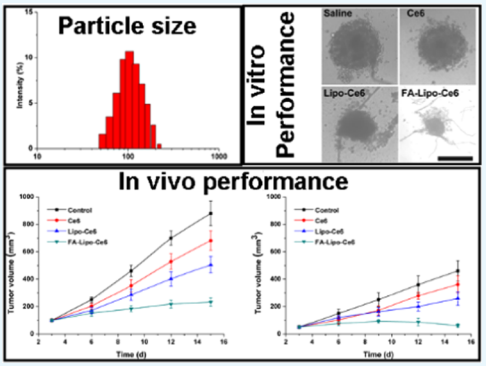

INTRODUCTION

The immunotherapy of cancer represents a class of novel treatments, including cancer vaccine, immune checkpoint therapy, and adoptive T cell therapy. In particular, compared with other methods, cancer vaccine with irreplaceable advantages, such as high accessibility and low cost, is widely treated as a better way for promising cancer treatment.[1,2] Recent studies have gradually revealed the critical role of dendritic cells (DCs) in the initiation of *T* cell response and the following immune cascades, which is indispensable for immunotherapy. As a result, many preceding researches have focused on exploring DC vaccines for the immunotherapy of cancers.[3,4] However, the previously developed formulations often require complex processing of blood products to afford required materials before further vaccination to the host.[5] Therefore, artificial on-demand DC vaccines that can minimize the processing complexity to provide a quick immune response are critical for excellent anticancer performance.[6]

In the past decade, the evolution of nanotechnology offers many powerful ways to prepare DC-based cancer vaccines.[7−10] Liposome (Lipo) is almost the most widely applied formulation in cancer therapy. It shows many advantages, including high biocompatibility, low cytotoxicity, and facile fabrication. Therefore, many drug delivery systems (DDSs) have employed Lipo as the skeleton that have shown satisfying outcomes.[11,12] According to previous reports, the combination of passive and positive targeting approaches is more potent than ordinary formulations.[13,14] Therefore, the construction of nanosized Lipo with positive targeting moiety conjugation is a promising way to realize cancer therapy. Moreover, it was also noted that many currently available formulations usually require repeated injections and high doses to meet acceptable therapeutic performance.[15−17] As a result, there is a great need for a novel platform capable of increasing the immunoreaction efficacy.[18−20]

Previous studies have shown promising potential of photodynamic therapy (PDT) to destroy the integrity of tumor tissues, during which the reactive oxygen species (ROS) is also capable of effectively killing cancer cells to induce significant apoptosis and to expose tumor-associated antigen (TAA).[21,22] Moreover, the natural inflammatory response characterized by a high level of ROS was also reported. As a result, it was suggested that the ROS produced by artificial PDT was capable of mimicking the inflammatory response of the body to employ the immune-related cells, including DC.[9,23] The unconsolidated tumor tissue after PDT was favorable for the distribution and penetration of DC for vaccination. The exposure of TAA was expected to activate DC to realize in situ vaccination, which was much more powerful than the traditional administration route and was also expected

Received: December 4, 2020
Accepted: January 14, 2021
Published: January 25, 2021

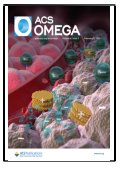

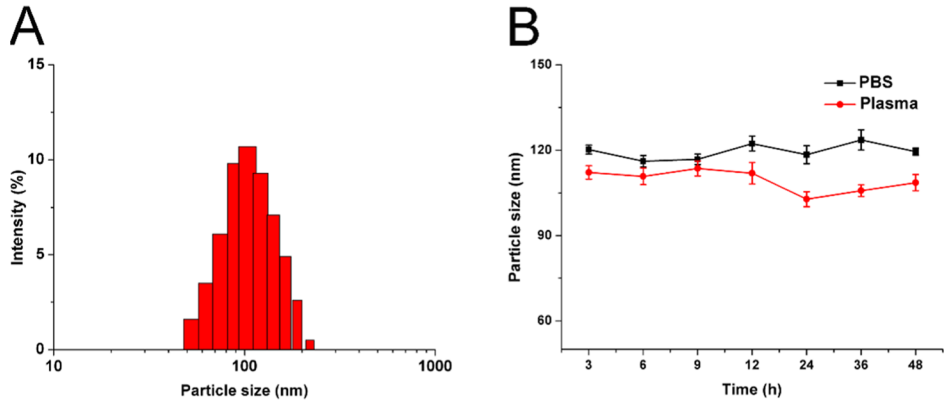

Figure 1. (A) Size distribution in FA-Lipo-Ce6. (B) Variations of FA-Lipo-Ce6 sizes upon incubation in phosphate-buffered saline (PBS) (pH 7.4) and mouse plasma (37 °C, 48 h). The results were expressed as the mean ± standard deviation (SD) of three independent experiments.

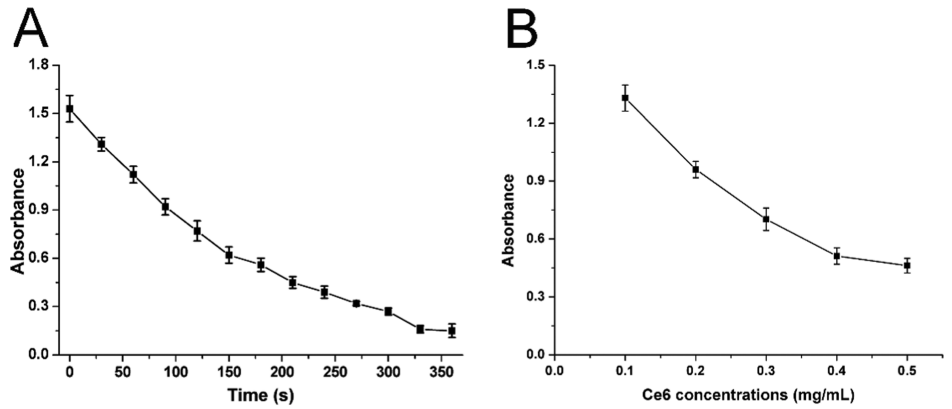

Figure 2. (A) Time-dependent changes of OD_{418nm} when FA-Lipo-Ce6 (Ce6 concentration: 0.1 mg/mL) was irradiated (1 W/cm^2). (B) Concentration-dependent changes in OD_{418nm} when FA-Lipo-Ce6 (Ce6 concentration: 0.1−0.5 mg/mL) was irradiated (1 W/cm^2) for 60 s. The results were expressed as the mean ± SD of three independent experiments.

to minimize the required dosage for effective immunotherapy.[4,24]

In this study, a folic acid (FA)-decorated Lipo vehicle (FA-Lipo) was developed to load chlorin e6 (FA-Lipo-Ce6) for PDT. The as-prepared DDS was expected to be a powerful in situ DC vaccine showing powerful immunotherapy in breast cancer models. The modified FA was expected to increase the tumor's targetability of the DDS upon administration. The Ce6 was expected to create ROS upon laser irradiation to damage the structure of tumor cells to effectively expose the TAA. Afterward, the DC cells recruited by the introduction of ROS (mimicking inflammation) processed and presented the antigen for a strong immune response.

RESULTS AND DISCUSSION

Preparation/Characterization of FA-Lipo-Ce6. The preparation of FA-Lipo-Ce6 was achieved using the rotary evaporation method in a one-pot approach. The Ce6 was loaded in the lipid matrix due to its hydrophilic nature, while the FA was modified onto the surface of the nanoparticles. As displayed in Figure 1A, the as-prepared FA-Lipo-Ce6 was fine nanoparticles with narrow size distribution at 100 nm. Previous reports noted that nanoparticles with size around 100 nm are optimal for making good use of the tumor-specific enhanced permeation and retention (EPR) effect than those with other sizes for promising tumor drug accumulation.[32−34] The drug loading capacity and encapsulation efficiency were determined as 6.92 and 91.03%, respectively.

To reveal the stability of FA-Lipo-Ce6, the nanoparticles were incubated in PBS/plasma for 48 h and the changes in particle sizes were selected as an indicator for stability. As shown in Figure 1B, in the entire period, the diameter of FA-Lipo-Ce6 only showed minor fluctuations (less than 10%), indicating that the stability of FA-Lipo-Ce6 could be well preserved at physiological conditions, which is beneficial to be a drug delivery platform for cancer therapy.

Although FA-Lipo-Ce6 can offer satisfactory protection to the loaded Ce6, it remains to be explored whether the packaged Ce6 can respond to the stimulation of laser to show photodynamic benefits. As a result, 1,3-diphenylisobenzofuran (DPBF) was employed to be an ROS probe to show ROS production profile of FA-Lipo-Ce6 upon laser irradiation. According to previous reports, DPBF can react with ROS to quench its UV absorption peak at 418 nm, and the degree of quenching is positively related to the amount of ROS in the environment. This is a convenient method to determine the ROS generation profile in the system. As displayed in Figure 2A, upon laser irradiation, the ROS concentration of FA-Lipo-Ce6 was significantly increased, as evidenced by the obvious quenching in OD_{418nm} (86.7% at 3 min of stimulation). Furthermore, results in Figure 2B also showed that the ROS generation of FA-Lipo-Ce6 is positively correlated with the concentration of Ce6. Both experiments indicated that Ce6 in

https://dx.doi.org/10.1021/acsomega.0c05924
ACS Omega 2021, 6, 3991−3998

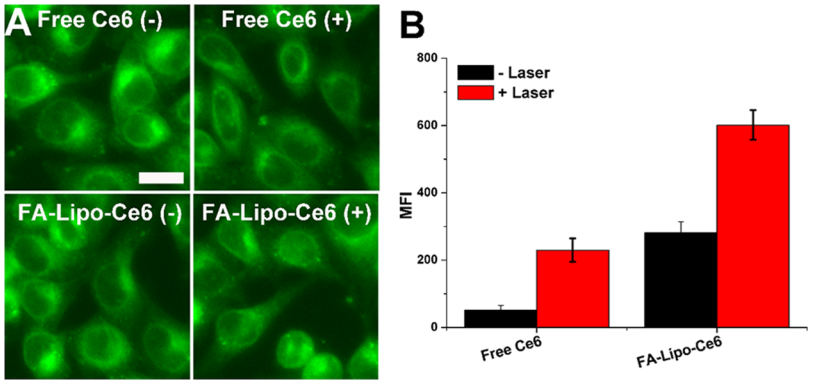

Figure 3. ROS generation capacity of FA-Lipo-Ce6. (A) Confocal laser scanning scope (CLSM) images of cells treated by free Ce6 or FA-Lipo-Ce6 with/without irradiation (1 W/cm^2, 5 min). The scale bar is 20 μm. (B) MFI of ROS in cells determined by flow cytometry. The results were expressed as the mean ± SD of three independent experiments.

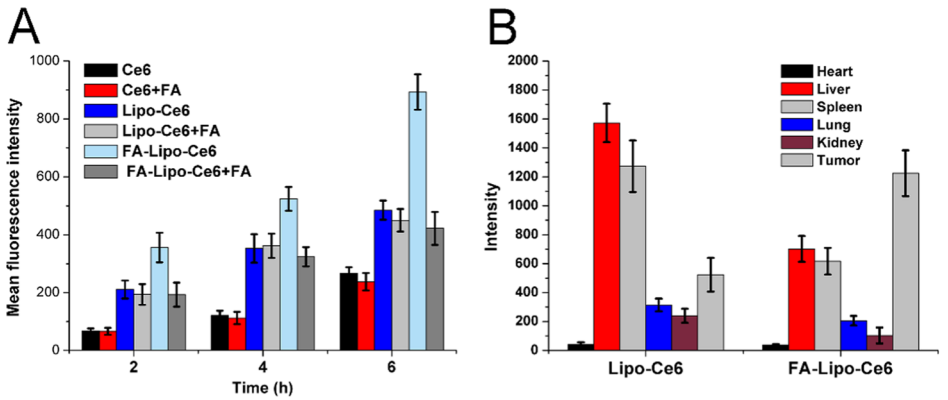

Figure 4. (A) Time-dependent cellular uptake of different formulations with/without pretreatment by FA. (B) Ex vivo MFI of tumors and other organs in mice after injection with Lipo-Ce6 and FA-Lipo-Ce6 for 48 h. The results were expressed as the mean ± SD of three independent experiments.

FA-Lipo-Ce6 retained the ability to produce ROS, which was beneficial to exert PDT for cancer therapy.

2′,7′-Dichlorodihydrofluorescein diacetate (DCFH-DA) can preferably penetrate into the cells without significant fluorescence. DCF is produced after degradation by intracellular lipase. Upon oxidation by ROS, the obtained DCF shows greatly enhanced fluorescence as compared to DCFH-DA, which offers the possibility to assess the cellular ROS profiles of FA-Lipo-Ce6. As shown in Figure 3A, the fluorescence of DCFH-DA in the free Ce6 group was weak without laser stimulation. As expected, the fluorescence increased after light irradiation, which suggested that laser stimulation is essential for the production of ROS. In contrast, the intracellular fluorescence intensity of the FA-Lipo-Ce6 group was higher than that of the free Ce6 group without laser irradiation, indicating that under the aid of DDS, Ce6 could more readily be internalized into cells. Similarly, after laser stimulation, the fluorescence signal in the FA-Lipo-Ce6 group was most significant than that in other groups, suggesting its best ROS creation profile. The results were further quantified using flow cytometry in Figure 3B; it was quantified that the ROS level in the FA-Lipo-Ce6 group was 3.86-fold of that in the free Ce6 group under laser irradiation, suggesting the effective delivery efficacy of FA-Lipo-Ce6 for PDT of cancers.

In Vitro Cellular Uptake and In Vivo Targeting. The drug delivery efficacy of different formulations in cells was explored. As displayed in Figure 4A, the cellular Ce6 intensity was positively related to the treating time. Moreover, as compared to two nanoparticles, the accumulation of free Ce6 in cells was the lowest among all three experimental groups, indicating that the introduction of DDS can significantly increase the accumulation of drugs in cells and was also consistent with previous reports.[35] Additionally, in the absence of FA, the FA-Lipo-Ce6 group showed a higher cellular Ce6 level than Lipo-Ce6 at all given time points. Interestingly, the intracellular Ce6 intensity of the FA-Lipo-Ce6 group decreased sharply after folic acid pretreatment, while the free Ce6 and Lipo-Ce6 groups exerted insignificant changes. These observations indicated that the FA decoration might enhance the internalization of FA-Lipo-Ce6 into 4T1 cells, possibly through the FA-mediated endocytosis.

To further verify the in vivo tumor-homing ability of FA-Lipo-Ce6 in 4T1 cells, the fluorescence distribution of Ce6 in major organs/tumors was obtained by in vitro imaging and the results are displayed in Figure 4B. The accumulation of Lipo-Ce6 in the tumor was poor with major retention in organs, particularly in the liver and spleen (reticuloendothelial system). In contrast, the Ce6 signal in the tumor tissue of the FA-Lipo-Ce6 group was much higher than that in organs, suggesting that the nontargeted distribution of Lipo-Ce6 was improved by the surface modification of Li and FA.

Anticancer Effect In Vitro. Next, we used the methyl thiazolyl tetrazolium (MTT) method to study the in vitro anticancer effect of different formulations on 4T1 cells. First, a

https://dx.doi.org/10.1021/acsomega.0c05924
ACS Omega 2021, 6, 3991−3998

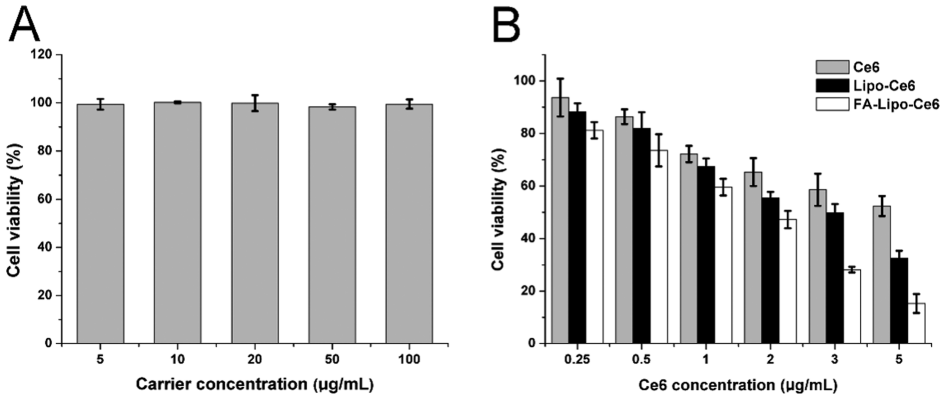

Figure 5. (A) Cytotoxicity effect (48 h) of FA-Lipo on 4T1 cells. (B) PDT-induced cytotoxicity effect of different formulations with different Ce6 concentrations (48 h) on 4T1 cells (400 mW/cm^2, 10 min). The results were expressed as the mean ± SD of three independent experiments.

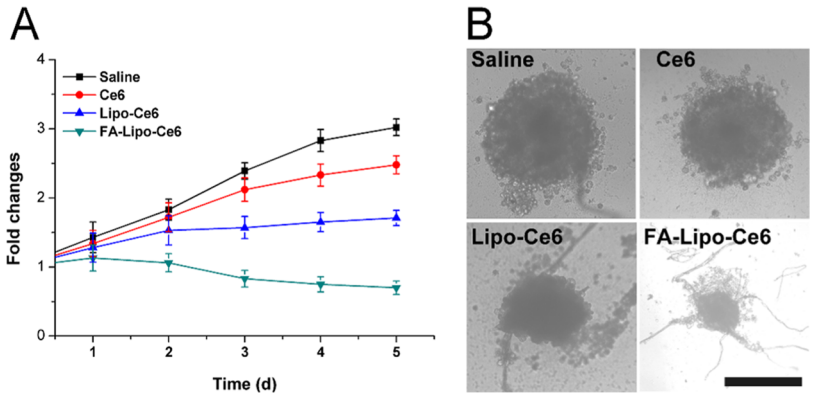

Figure 6. Changes in MCTS volume (A) and the images (B) of MCTS in different groups at the end of the test. The results were expressed as the mean ± SD of three independent experiments.

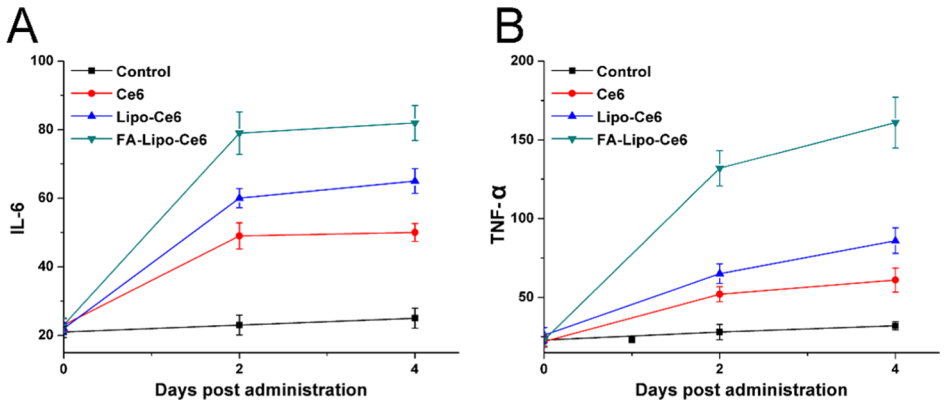

Figure 7. Time-dependent changes in IL-6 (A) and TNF-α (B) levels in mouse sera from mice after different treatments. The results were expressed as the mean ± SD of three independent experiments.

blank vector without drugs was cultured with the cells to study its biocompatibility. As displayed in Figure 5A, at 48 h after incubation (carrier concentration: 100 μg/mL), the viability of 4T1 cells was not significantly reduced. These results indicate that FA-Lipo is highly biocompatible and suitable to be a drug delivery vehicle.

Thereafter, the anticancer effects of the drug-loaded FA-Lipo-Ce6 were evaluated employing free Ce6 and Lipo-Ce6 as negative controls. According to Figure 5B, the PDT effects of all Ce6-containing formulations under the given laser conditions positively correlated with the concentration of Ce6. Furthermore, unlike DDSs, free Ce6 showed an inferior anticancer effect, which was in line with the cellular uptake assay that DDS showed a positive effect on drug accumulation in cells.[36,37] Most importantly, compared to Lipo-Ce6, the advantages of FA-Lipo-Ce6 were significantly enhanced under all given Ce6 concentrations. In particular, at a concentration of 5 μg/mL, the viability of cells upon PDT was less than 15%, which was optimal among all groups.

Multicellular tumor spheroid (MCTS), constructed by fibroblasts and cancer cells, is widely adopted in in vitro experiments to mimic solid tumors and to explore the anticancer performance of DDS. From Figure 6A, it was observed that cells treated with saline showed a continual

https://dx.doi.org/10.1021/acsomega.0c05924
ACS Omega 2021, 6, 3991−3998

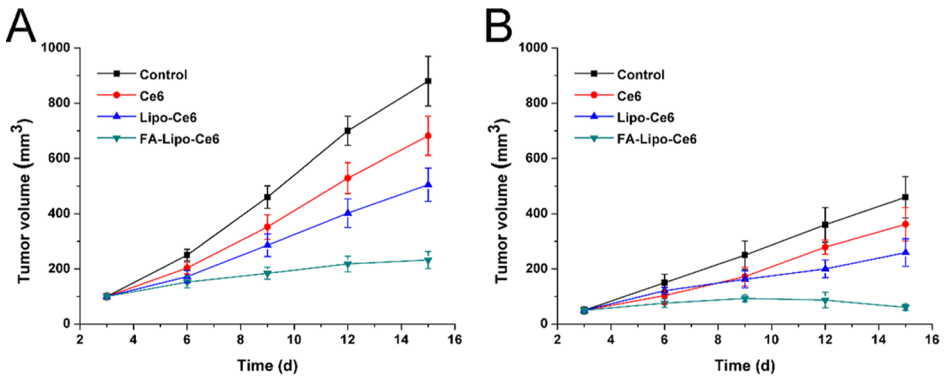

Figure 8. In vivo anticancer effect of different treatments on C57BL/6 mice-bearing 4T1 tumor. The time-dependent changes in tumor volume at (A) primary and (B) distant tumors were recorded. The temperature upon irradiation was around 40 °C. The results were expressed as the mean ± SD of six independent experiments.

increase of MCTS volume and reached a final volume of 3.2 times as compared to the original one. In contrast, the growth of MCTS subjected to PDT was significantly inhibited. As noted, in line with the results of the MTT assay, FA-Lipo-Ce6-treated MCTS showed only 75% of initial volume at the end of the test, indicating the optimal anticancer performance. The results of optical observations in Figure 6B also showed similar conclusions. It was observed that MCTS after PDT treatment has structural damage and cell apoptosis, and the MCTS in the FA-Lipo-Ce6 group has the smallest volume and the most significant structural damage.

In Situ Vaccination of DC and Immunoreaction. Results from previous studies have shown that PDT can destroy the integrity of cells and also mimic the inflammation process in vivo. As a result, upon PDT, the tumor tissue was expected to expose sufficient TAA and employ the DC for in situ vaccination, resulting in strong immune responses. Therefore, two representative cytokines (IL-6 and TNF-α) were selected and their plasma concentrations were measured at different time points after PDT using an ELISA kit. It was reported that the activated DC can secrete IL-6 and TNF-α, which can therefore become indicators to reflect the activation of DC.[38] As displayed in Figure 7, while the control group showed insignificant changes in plasma concentrations of IL-6 and TNF-α, these two indicators in the PDT groups were elevated significantly and maintained at a similar level until 4 days post treatment. These results strongly indicated the activation of DC cells upon PDT, which persistently released cytokines for strong immune responses. As expected, FA-Lipo-Ce6 after PDT showed the highest cytokine levels among all tested groups, indicating its capability to be an effective in situ vaccine for strong immune response.

In Vivo Anticancer Study. To explore the relation of in situ DC vaccine and the in vivo anticancer benefits, 4T1 tumors were inoculated on both sides of the mice with the larger one (inoculated with more 4T1 cells) as the primary tumor and the other as the distant tumor. The primary tumor was subjected to PDT, and both the volume of primary/distant tumors was recorded at day 3 and repeated every 3 days in 15 days. As shown in Figure 8, both primary and distant tumors were obviously inhibited during the test in the FA-Lipo-Ce6 group (232 mm^3 of primary tumor and 61 mm^3 of distant tumor) after PDT as compared to those in the control group. However, tumors in the Lipo-Ce6 group persistently increased to reach the final tumor volumes of 505 mm^3 (primary) and 259 mm^3 (distant), respectively, indicating the importance of FA modification in the increase of tumor homing of the DDS. However, the promoted T cell (such as CD8+ and CD4+) populations in the spleen should be given to further confirm this conclusion, which might be displayed in our future work. In all, these results strongly suggested the significance of in situ DC vaccination of FA-Lipo-Ce6 for the effective therapy of breast cancer.

CONCLUSIONS

In this study, we developed FA-modified Lipo (FA-Lipo) as a drug delivery vehicle for the loading of Ce6 (FA-Lipo-Ce6), which served as a powerful in situ DC vaccine for immunotherapy of breast cancer. Our results suggested that the stability and biocompatibility of FA-Lipo-Ce6 were acceptable and the FA modification effectively increased the accumulation of Ce6 in 4T1 cells, which in turn increased the generated ROS level after laser irradiation. Based on MTT and MCTS assays, it was confirmed that FA-Lipo-Ce6 showed optimal in vitro anticancer assay. Moreover, the plasma level of DC-related cytokines (IL-6 and TNF-α) suggested that FA-Lipo-Ce6 can significantly boost the activation of DC for a strong immune response, which showed the best in vivo anticancer benefits than other groups, indicating its potential to be a novel way for effective cancer therapy.

EXPERIMENTAL SECTION

Materials. Phosphatidylethanolamines (DSPEs), cholesterol, 1,3-diphenylisobenzofuran (DPBF), methyl thiazolyl tetrazolium (MTT), 2′,7′-dichlorodihydrofluorescein diacetate (DCFH-DA), chlorins e6 (Ce6), folic acid (FA), Triton X-100, paraformaldehyde cholesterol, and paraformaldehyde were provided by Sigma-Aldrich (St. Louis, MO). DSPE-PEG and FA−DSPE-PEG were offered by Sangon Biotech (Shanghai, China).

Cell and Animal Models. 4T1 (mouse breast carcinoma cell line) and NIH3T3 (mouse embryonic fibroblast) cell lines were obtained from the Shanghai Model Cell Center (Shanghai, China). All cell lines were cultured using the standard protocols mentioned in previous reports.[25] The multicellular tumor spheroid (MCTS) was established according to the previous report.[19] Female C57BL/6J mice (6−8 weeks) were purchased from the Wuhan Model Animal Center (Wuhan, China) and raised under standard conditions. The establishment of the 4T1 tumor-bearing mice model was in line with the previous report.[26] In brief, $6/2 \times 10^5$ 4T1 cells

https://dx.doi.org/10.1021/acsomega.0c05924
ACS Omega 2021, 6, 3991−3998

were inoculated subcutaneously to the right/left flank of the mice to generate primary/distant tumors. All animal procedures in this study were reviewed and approved by the Institutional Ethics Committee of the Huazhong University of Science and Technology.

Preparation of FA-Lipo-Ce6. The liposome was constructed using the rotary evaporation method. In brief, DSPE (10 mg), cholesterol (2 mg), DSPE-PEG and FA−DSPE-PEG (2 mg), and Ce6 (3 mg) were dissolved in appropriate amounts of mixed solution (chloroform/ethanol = 1:1, v/v) in a flask. Afterward, the solution was evaporated under vapor to obtain a thin layer. Finally, 10 mL of PBS (pH 7.4) was added into the flask under rotation to obtain a transparent solution, which was FA-Lipo-Ce6.

FA-unmodified Lipo-Ce6 was employed as a control in the following study and was prepared using a similar method without the addition of FA−DSPE-PEG.

Characterization. The size distribution of FA-Lipo-Ce6 was determined by particle sizing system (Nano9200, Hairuixin, China) in PBS/plasma for 48 h for stability assessment.[27] The morphology was shown by transmission electron microscope (TEM, Hitachi-2100, Hitachi, Japan).

The serum was collected from the tested mice at prearranged time points and subjected to centrifugation (CR21, Hitachi, Japan, 10 000 g, 30 min) to obtain supernatants. IL-6 and TNF-α levels in the serum supernatant were determined by ELISA kit (Omega) as instructed.

Drug Release and ROS Generation. The drug release of Ce6 from FA-Lipo-Ce6 was determined using the previously reported protocol.[28] The ROS generation was assessed using DPBF. In brief, 20 μL of DPBF (10 mM) was incubated with FA-Lipo-Ce6 to give a uniform solution. After that, the mixture was subjected to laser irradiation (680 nm, 1 W/cm^2) and OD_{418nm} was recorded by a UV spectrophotometer (TU-1800, Persee, Beijing China).

In Vitro Anticancer Study. Drug-free Lipo at a concentration between 5 and 100 μg/mL and FA-Lipo-Ce6 at a drug concentration between 0.25 and 5 μg/mL were incubated with 4T1 cells for 48 h. The laser irradiation was performed at 4 h post incubation (680 nm, 400 mW/cm^2 for 10 min). At the end of treatment, cell viability was assessed by a standard MTT assay according to the previous report.[29] Moreover, MCTS was incubated with free Ce6, Lipo-Ce6, and FA-Lipo-Ce6 (Ce6 concentration of 5 μg/mL) for 24 h and then treated with laser as mentioned above. The volume changes of MCTS were monitored for 5 days.

Intracellular Uptake and ROS Generation. 4T1 cells were pretreated with and without excess FA (1 mM) for 2 h and then incubated with free Ce6, Lipo-Ce6, and FA-Lipo-Ce6 for different time intervals (2, 4, and 6 h). Afterward, cells were collected and analyzed by flow cytometer (FCM, ACEA NovoCyte, Agilent, California).

In addition, cells were treated with different formulations for 4 h and then loaded with an ROS probe (DCFH-DA, 25 mM) for 0.5 h in dark. After treating with and without laser irradiation (400 mW/cm^2, 5 min), cells were viewed by a confocal laser scanning scope (CLSM, A1R MP, Nikon, Tokyo, Japan).

In Vivo Drug Distribution. 4T1 tumor-bearing mice with only primary tumors were administered intravenously with Lipo-Ce6 and FA-Lipo-Ce6. After 48 h of distribution, mice were sacrificed and the organs/tumors were collected to reveal the accumulation of Ce6 using in vivo imaging technic (In-Vivo Xtreme, Bruker, Germany).[30]

In Vivo Anticancer Assay. Every six tumor-bearing mice were randomly employed as one group and given saline (as control), free Ce6, Lipo-Ce6, and FA-Lipo-Ce6 (5 mg/kg Ce6) intravenously. The primary tumor was treated with a 680 nm laser irradiation (100 mW/cm^2, 20 min) at 24 h post drug administration. The administration was repeated every 2 days for 2 times.[31] The tumor volumes and body weight of all mice were recorded at day 3 and repeated every 3 days for a period of 15 days.

AUTHOR INFORMATION

Corresponding Author

Jianyuan Yang − *Department of Thyroid and Breast Surgery, The Central Hospital of Wuhan, Tongji Medical College, Huazhong University of Science and Technology, Wuhan 430014, China;* orcid.org/0000-0001-6737-2982; Email: jianyuanyang02@163.com

Authors

Hong Pan − *Department of Thyroid and Breast Surgery, The Central Hospital of Wuhan, Tongji Medical College, Huazhong University of Science and Technology, Wuhan 430014, China*

Hongyan Shi − *Department of Thyroid and Breast Surgery, The Central Hospital of Wuhan, Tongji Medical College, Huazhong University of Science and Technology, Wuhan 430014, China*

Peng Fu − *Department of Thyroid and Breast Surgery, The Central Hospital of Wuhan, Tongji Medical College, Huazhong University of Science and Technology, Wuhan 430014, China*

Pengfei Shi − *Department of Thyroid and Breast Surgery, The Central Hospital of Wuhan, Tongji Medical College, Huazhong University of Science and Technology, Wuhan 430014, China*

Complete contact information is available at: https://pubs.acs.org/10.1021/acsomega.0c05924

Author Contributions

‡H.P. and H.S. contributed equally to this work.

Notes

The authors declare no competing financial interest.

ACKNOWLEDGMENTS

The authors acknowledge the language help from Letpub.

REFERENCES

(1) Zhu, G.; Lynn, G. M.; Jacobson, O.; Chen, K.; Liu, Y.; Zhang, H.; Ma, Y.; Zhang, F.; Tian, R.; Ni, Q. Albumin/vaccine nanocomplexes that assemble in vivo for combination cancer immunotherapy. *Nat. Commun.* **2017**, *8*, No. 1954.

(2) Zhang, X.; Wang, J.; Chen, Z.; Hu, Q.; Wang, C.; Yan, J.; Dotti, G.; Huang, P.; Gu, Z. Engineering PD-1-presenting platelets for cancer immunotherapy. *Nano Lett.* **2018**, *18*, 5716−5725.

(3) Zhang, Z.; Qian, H. Q.; Huang, J.; Sha, H. Z.; Zhang, H.; Yu, L. X.; Liu, B. R.; Hua, D.; Qian, X. P. Anti-EGFR-iRGD recombinant protein modified biomimetic nanoparticles loaded with gambogic acid to enhance targeting and antitumor ability in colorectal cancer treatment. *Int. J. Nanomed.* **2018**, *13*, 4961−4975.

(4) He, H.; Zhu, R.; Sun, W.; Cai, K.; Chen, Y.; Yin, L. Selective cancer treatment via photodynamic sensitization of hypoxia-responsive drug delivery. *Nanoscale* **2018**, *10*, 2856−2865.

(5) Restifo, N. P.; Dudley, M. E.; Rosenberg, S. A. Adoptive immunotherapy for cancer: harnessing the T cell response. *Nat. Rev. Immunol.* **2012**, *12*, 269−281.
(6) Palucka, K.; Banchereau, J. Cancer immunotherapy via dendritic cells. *Nat. Rev. Cancer* **2012**, *12*, 265−277.
(7) Peng, J.; Xiao, Y.; Li, W.; Yang, Q.; Tan, L.; Jia, Y.; Qu, Y.; Qian, Z. Photosensitizer micelles together with IDO inhibitor enhance cancer photothermal therapy and immunotherapy. *Adv. Sci.* **2018**, *5*, No. 1700891.
(8) Meng, Z.; Zhou, X.; Xu, J.; Han, X.; Dong, Z.; Wang, H.; Zhang, Y.; She, J.; Xu, L.; Wang, C.; Liu, Z. Light-Triggered In Situ Gelation to Enable Robust Photodynamic-Immunotherapy by Repeated Stimulations. *Adv. Mater.* **2019**, *31*, No. 1900927.
(9) He, C.; Duan, X.; Guo, N.; Chan, C.; Poon, C.; Weichselbaum, R. R.; Lin, W. Core-shell nanoscale coordination polymers combine chemotherapy and photodynamic therapy to potentiate checkpoint blockade cancer immunotherapy. *Nat. Commun.* **2016**, *7*, No. 12499.
(10) Cho, N.-H.; Cheong, T.-C.; Min, J. H.; Wu, J. H.; Lee, S. J.; Kim, D.; Yang, J.-S.; Kim, S.; Kim, Y. K.; Seong, S.-Y. A multifunctional core−shell nanoparticle for dendritic cell-based cancer immunotherapy. *Nat. Nanotechnol.* **2011**, *6*, 675.
(11) Aghdam, M. A.; Bagheri, R.; Mosafer, J.; Baradaran, B.; Hashemzaei, M.; Baghbanzadeh, A.; de la Guardia, M.; Mokhtarzadeh, A. Recent advances on thermosensitive and pH-sensitive liposomes employed in controlled release. *J. Controlled Release* **2019**, *315*, 1−22.
(12) Manna, S.; Wu, Y.; Wang, Y.; Koo, B.; Chen, L.; Petrochenko, P.; Dong, Y.; Choi, S.; Kozak, D.; Oktem, B.; et al. Probing the mechanism of bupivacaine drug release from multivesicular liposomes. *J. Controlled Release* **2019**, *294*, 279−287.
(13) Tan, L. W.; Ma, B. Y.; Qian, Zhao.; Lan, Zhang.; Chen, L. J.; Peng, J. R.; Qian, Z. Y. Toxicity Evaluation and Anti-Tumor Study of Docetaxel Loaded mPEG-Polyester Micelles for Breast Cancer Therapy. *J. Biomed. Nanotechnol.* **2017**, *13*, 393−408.
(14) Vijayavenkataraman, S.; Zhang, S.; Lu, W. F.; Fuh, J. Y. H. Electrohydrodynamic-jetting (EHD-jet) 3D-printed functionally graded scaffolds for tissue engineering applications. *J. Mater. Res.* **2018**, *33*, 1999−2011.
(15) Li, H.; Zhao, Y.; Jia, Y.; Qu, C.; Li, J. Covalently assembled dopamine nanoparticle as an intrinsic photosensitizer and pH-responsive nanocarrier for potential application in anticancer therapy. *Chem. Commun.* **2019**, *55*, 15057−15060.
(16) Peng, Y.; Huang, J.; Xiao, H.; Wu, T.; Shuai, X. Codelivery of temozolomide and siRNA with polymeric nanocarrier for effective glioma treatment. *Int. J. Nanomed.* **2018**, *13*, 3467.
(17) Wang, C.; Chen, S.; Bao, L.; Liu, X.; Hu, F.; Yuan, H. Size-Controlled Preparation and Behavior Study of Phospholipid−Calcium Carbonate Hybrid Nanoparticles. *Int. J. Nanomed.* **2020**, *15*, 4049−4062.
(18) Mei, K.-C.; Liao, Y.-P.; Jiang, J.; Chiang, M.; Khazaieli, M.; Liu, X.; Wang, X.; Liu, Q.; Chang, C. H.; Zhang, X.; et al. Liposomal delivery of mitoxantrone and a cholesteryl indoximod prodrug provides effective chemo-immunotherapy in multiple solid tumors. *ACS Nano* **2020**, *14*, 13343−13366.
(19) Wang, C.; Shi, X.; Song, H.; Zhang, C.; Wang, X.; Huang, P.; Dong, A.; Zhang, Y.; Kong, D.; Wang, W. Polymer-lipid hybrid nanovesicle-enabled combination of immunogenic chemotherapy and RNAi-mediated PD-L1 knockdown elicits antitumor immunity against melanoma. *Biomaterials* **2021**, *268*, No. 120579.
(20) Zhou, Z.; Wu, H.; Yang, R.; Xu, A.; Zhang, Q.; Dong, J.; Qian, C.; Sun, M. GSH depletion liposome adjuvant for augmenting the photothermal immunotherapy of breast cancer. *Sci. Adv.* **2020**, *6*, No. eabc4373.
(21) Ni, J.; Sun, Y.; Song, J.; Zhao, Y.; Gao, Q.; Li, X. Artificial Cell-Mediated Photodynamic Therapy Enhanced Anticancer Efficacy through Combination of Tumor Disruption and Immune Response Stimulation. *ACS Omega* **2019**, *4*, 12727−12735.
(22) Yang, D.; Yang, G.; Sun, Q.; Gai, S.; He, F.; Dai, Y.; Zhong, C.; Yang, P. Carbon-Dot-Decorated TiO2 Nanotubes toward Photodynamic Therapy Based on Water-Splitting Mechanism. *Adv. Healthcare Mater.* **2018**, *7*, No. 1800042.
(23) Yang, J.; Teng, Y.; Fu, Y.; Zhang, C. Chlorins e6 loaded silica nanoparticles coated with gastric cancer cell membrane for tumor specific photodynamic therapy of gastric cancer. *Int. J. Nanomed.* **2019**, *14*, 5061.
(24) Ma, S.; Zhou, J.; Zhang, Y.; Yang, B.; He, Y.; Tian, C.; Xu, X.; Gu, Z. An Oxygen Self-sufficient Fluorinated Nanoplatform for Relieved Tumor Hypoxia and Enhanced Photodynamic Therapy of Cancers. *ACS Appl. Mater. Interfaces* **2019**, *11*, 7731−7742.
(25) Negi, L. M.; Talegaonkar, S.; Jaggi, M.; Verma, A. K. Hyaluronated imatinib liposomes with hybrid approach to target CD44 and P-gp overexpressing MDR cancer: an in-vitro, in-vivo and mechanistic investigation. *J. Drug Targeting* **2019**, *27*, 183−192.
(26) Li, C.; Yang, X.-Q.; An, J.; Cheng, K.; Hou, X.-L.; Zhang, X.-S.; Hu, Y.-G.; Liu, B.; Zhao, Y.-D. Red blood cell membrane-enveloped O2 self-supplementing biomimetic nanoparticles for tumor imaging-guided enhanced sonodynamic therapy. *Theranostics* **2020**, *10*, 867.
(27) Ding, X.; Xu, X.; Zhao, Y.; Zhang, L.; Yu, Y.; Huang, F.; Yin, D.; Huang, H. Tumor targeted nanostructured lipid carrier co-delivering paclitaxel and indocyanine green for laser triggered synergetic therapy of cancer. *RSC Adv.* **2017**, *7*, 35086−35095.
(28) Zhu, Y.; Yu, F.; Tan, Y.; Hong, Y.; Meng, T.; Liu, Y.; Dai, S.; Qiu, G.; Yuan, H.; Hu, F. Reversing activity of cancer associated fibroblast for staged glycolipid micelles against internal breast tumor cells. *Theranostics* **2019**, *9*, 6764−6779.
(29) Wang, P.; Wang, X.; Luo, Q.; Li, Y.; Lin, X.; Fan, L.; Zhang, Y.; Liu, J.; Liu, X. Fabrication of red blood cell-based multimodal theranostic probes for second near-infrared window fluorescence imaging-guided tumor surgery and photodynamic therapy. *Theranostics* **2019**, *9*, 369.
(30) Silva, J. S. F.; Silva, J. Y. R.; de Sa, G. F.; Araujo, S. S.; Gomes, M. A.; Ronconi, C. M.; Santos, T. C.; Junior, S. A. Multifunctional System Polyaniline-Decorated ZIF-8 Nanoparticles as a New Chemo-Photothermal Platform for Cancer Therapy. *ACS Omega* **2018**, *3*, 12147−12157.
(31) Zhang, X.; Tan, X.; Zhang, D.; Liao, N.; Zheng, Y.; Zheng, A.; Zeng, Y.; Liu, X.; Liu, J. A cancer cell specific targeting nanocomplex for combination of mRNA-responsive photodynamic and chemotherapy. *Chem. Commun.* **2017**, *53*, 9979−9982.
(32) Hu, R.; Zheng, H.; Cao, J.; Davoudi, Z.; Wang, Q. Synthesis and In Vitro Characterization of Carboxymethyl Chitosan-CBA-Doxorubicin Conjugate Nanoparticles as pH-Sensitive Drug Delivery Systems. *J. Biomed. Nanotechnol.* **2017**, *13*, 1097−1105.
(33) Gao, F.; Zhang, J. M.; Fu, C. M.; Xie, X. M.; Peng, F.; You, J. S.; Tang, H. L.; Wang, Z. Y.; Li, P.; Chen, J. P. iRGD-modified lipid-polymer hybrid nanoparticles loaded with isoliquiritigenin to enhance anti-breast cancer effect and tumor-targeting ability. *Int. J. Nanomed.* **2017**, *12*, 4147−4162.
(34) Brillault, L.; Jutras, P. V.; Dashti, N.; Thuenemann, E. C.; Morgan, G.; Lomonossoff, G. P.; Landsberg, M. J.; Sainsbury, F. Engineering Recombinant Virus-like Nanoparticles from Plants for Cellular Delivery. *ACS Nano* **2017**, *11*, 3476−3484.
(35) Wang, J.; Tao, S.; Jin, X.; Song, Y.; Zhou, W.; Lou, H.; Zhao, R.; Wang, C.; Hu, F.; Yuan, H. Calcium Supplement by Tetracycline guided amorphous Calcium Carbonate potentiates Osteoblast promotion for Synergetic Osteoporosis Therapy. *Theranostics* **2020**, *10*, 8591.
(36) Palko-Łabuz, A.; Środa-Pomianek, K.; Wesołowska, O.; Kostrzewa-Susłow, E.; Uryga, A.; Michalak, K. MDR reversal and pro-apoptotic effects of statins and statins combined with flavonoids in colon cancer cells. *Biomed. Pharmacother.* **2019**, *109*, 1511−1522.
(37) Luesakul, U.; Puthong, S.; Neamati, N.; Muangsin, N. pH-responsive selenium nanoparticles stabilized by folate-chitosan delivering doxorubicin for overcoming drug-resistant cancer cells. *Carbohydr. Polym.* **2018**, *181*, 841−850.
(38) Da Silva, C. G.; Camps, M. G. M.; Li, T. M. W. Y.; Zerrillo, L.; Löwik, C. W.; Ossendorp, F.; Cruz, L. J. Effective chemo-

https://dx.doi.org/10.1021/acsomega.0c05924
ACS Omega 2021, 6, 3991−3998

immunotherapy by co-delivery of doxorubicin and immune adjuvants in biodegradable nanoparticles. *Theranostics* **2019**, *9*, 6485.

https://dx.doi.org/10.1021/acsomega.0c05924
ACS Omega 2021, 6, 3991−3998